Available online at www.sciencedirect.com
SCIENCE DIRECT
Journal of Controlled Release 112 (2006) 88–95
journal of controlled release
www.elsevier.com/locate/jconrel

Study on drug release behaviour of CDHA/chitosan nanocomposites—Effect of CDHA nanoparticles

Tse-Ying Liu [a], San-Yuan Chen [a,*], Jo-Hao Li [a], Dean-Mo Liu [b]

[a] *Department of Materials Science and Engineering, National Chiao Tung University, 1001 Ta-hsueh Rd., Hsinchu, Taiwan, ROC*
[b] *ApaMatrix Technologies Inc. 7431 Bates Road, Richmond, British Columbia, Canada*

Received 11 March 2005; accepted 31 January 2006
Available online 10 March 2006

Abstract

To explore the effect of nanofiller–polymer interaction on the drug release behaviour from a monolithic membrane prepared by Ca-deficient hydroxyapatite (CDHA)/chitosan nanocomposite, release kinetics was investigated in terms of different synthetic processes, i.e. in situ and ex situ routes, and various amounts of CDHA. It was found that a higher value of diffusion exponent (n) was obtained for the membranes in situ synthesized compared with those ex situ prepared. In addition, the n value of the membranes in situ synthesized increased with increasing CDHA amount, which remained in the range below 10 wt.%. However, as CDHA content exceeded 30%, the n value remained constant. It indicates that the drug diffusion mechanism is altered by the CDHA–chitosan interaction which is strongly influenced by both the synthesis process and the concentration of the CDHA nanofiller in the membrane. On the other hand, a lower permeability (P) value of the membranes was observed for those prepared via the in situ process. Furthermore, P value decreased and increased with increasing CDHA amount in the range below and above 10 wt.%, respectively. It demonstrates that CDHA nanofillers act either diffusion barrier or diffusion enhancer for the CDHA/chitosan membranes, which is determined by the concentration of CDHA nanofiller and the synthesis route of nanocomposite.

Keywords: Chitosan; Ca-deficient hydroxyapatite; Nanocomposite; Drug release; In situ process

1. Introduction

Chitosan (CS) has been widely used as a scaffolding material in tissue engineering [1], orthopedic implants [2] and drug delivery vehicles [3] for many years because of its low price and outstanding characters, such as osteoconductivity, biodegradability, and biocompatibility. Nevertheless, chitosan lacks sufficient mechanical strength, which restricts its uses for load-bearing applications, especially in orthopedics. Many studies have attempted to improve its mechanical strength by incorporating calcium phosphate bioactive ceramic such as hydroxyapatite (HAp, $Ca_{10}(PO_4)_6(OH)_2$) and β-tricalcium phosphate (β-TCP, $Ca_3(PO_4)_2$) [4,5]. However, natural bone mineral has essentially a calcium-deficient apatitic structure (Ca-deficient hydroxyapatite, CDHA) with a Ca/P ratio of about 1.5, which is compositionally similar to tricalcium phosphates (Ca/P = 1.5) and structurally similar to stoichiometric hydroxyapatite (Ca/P = 1.67). Therefore, CDHA is considered to be a candidate material with respect to both mechanical reinforcement and biological activity for orthopedic application.

The key to success in using macroporous implantable devices for osteogenesis is not only the suitable matrix with sufficient bioactivity and mechanical strength for osteogenic progenitor cells, but also the sustained release of antibiotics and growth factors to eliminate infection and insure osteoblast differentiation, respectively [3,6]. Up to now, many studies have been done for the influence of hydroxyapatite nanoparticles on the mechanical properties of CS/HAp nanocomposites for orthopedic use [7,8]. However, the role of CDHA nano-crystals in drug release behaviour of chitosan-based composite has rarely been found in the literature. In order to enhance the therapeutic efficiency of a bioactive agent via manipulating its release profiles, it is necessary to explore the effect of CDHA nano-crystals on the drug release mechanism of the CS-based polymeric matrix.

* Corresponding author. Tel.: +886 3 5731818; fax: +886 3 5725490.
E-mail address: sychen@cc.nctu.edu.tw (S.-Y. Chen).

0168-3659/$ - see front matter © 2006 Elsevier B.V. All rights reserved.
doi:10.1016/j.jconrel.2006.01.017

Generally, drug release kinetics of polymeric drug delivery system is usually characterized by membrane permeability (P) and diffusion exponent (n), which are employed to describe the release behaviours of reservoir (membrane) systems and the diffusion mechanism for monolithic (matrix) systems, respectively [9]. Furthermore, both indexes in polymer-based materials are strongly dependent on crystallinity, plasticization, glass transition temperature (T_g) and swelling of the polymer vehicle, which are also affected by the presence of nanofillers [10–12]. Most researchers found an increase in T_g as a function of nanofiller content [13,14]. On the contrary, a decrease in T_g with increase in nanofiller was also reported [12,15]. Furthermore, the influence of filler on resulting crystallinity of the polymeric phase has not been consistently reported. Some reported that the nanofiller acted as a nucleation agent to enhance the crystallinity of semi-crystalline polymer [11]. However, some suggested that the nanofiller could retard the evolution of crystalline structure within the polymeric domains of the composite [16]. These arguments arise due to various extents of polymer–filler interaction in different composite systems [16,17]. In order to classify the role of polymer–filler interaction in the drug release behaviours of CDHA/CS nanocomposites, the in situ preparation process was employed and expected to enhance polymer–filler interaction to alter the diffusion mechanism of CDHA/chitosan composite [18].

In this work, with the aim of studying the role of polymer–filler interaction in the drug release behaviours of CDHA/CS nanocomposites, in situ incorporation of CDHA nanoparticles, i.e. CDHA synthesized in the presence of chitosan, was employed. For comparison, ex situ synthetic process was also used. In other words, CDHA nanofiller was synthesized first and then added into the chitosan solution. Membrane permeability and diffusion exponent of CDHA/CS nanocomposites with various CDHA contents were systematically investigated to explore the influence of CDHA nanofillers on the drug release behaviour and the corresponding release mechanism.

2. Experimental methods

2.1. CDHA/CS nanocomposite membrane preparation

In this study, the CDHA/CS nanocomposite membranes with various CDHA contents were prepared via in situ and ex situ processes to characterize the influence of nanofiller and polymer–filler interaction on drug delivery behaviour. CS with 215 k molecular weight and 80% degree of deacetylation was supplied by Aldrich-Sigma. CS solution of 1% (w/v) was first prepared by dissolving CS powder in 10% (v/v) acetic acid solution. For ex situ processes, CDHA nanoparticles were first synthesized by mixing $Ca(CH_3COO)_2$ aqueous solution with H_3PO_4 aqueous solution. The pH value was kept at 7.5 by the addition of NaOH solution (1 M). The un-reacted precursors in the resulting CDHA suspension were removed by repeated precipitation and distilled-water (DI water) washing for three times. The resulting CDHA/DI water suspension was added into the CS solution to form CDHA/CS suspension. For the in situ process, H_3PO_4 aqueous solution (0.16 M) was first added into the CS solution, and $Ca(CH_3COO)_2$ aqueous solution (0.25 M) was then added into this mixture solution. The pH value was also kept at 7.5 by adding NaOH solution (1 M). The composite membranes with the volume ratios of CDHA/CS controlled at 95/5, 90/10, 70/30 and 50/50 for both in situ and ex situ processes (see Table 1). Subsequently, these CDHA/CS suspensions were poured into Petri dish to form CDHA/CS membranes after drying at room temperature for 7 days.

2.2. Material characterization

The volume ratio of CDHA/CS was confirmed by thermogravitational analysis (TGA, Perkin Elmer). The crystallographic phase of CDHA/CS composites was identified by X-ray diffractometer (XRD, M18XHF, Mac Science, Tokyo, Japan). The morphology of both composite membranes and CDHA nano-crystals was observed by using scanning electron microscopy (SEM, Hitachi S4000) and transmission electron microscopy (TEM, JEOL-2000FX). Dynamic mechanical analysis (DMA) was performed using a TA Instruments 2980 dynamic mechanical analyzer from −130 to 210 °C with a frequency of 1 Hz and a heating rate of 2 °C/min.

2.3. Determination of diffusion exponent for drug-loaded matrix system

Vitamin B_{12} (Sigma, V-2876) is a water-soluble agent with low molecular weight (1355 Da), small molecular size and negligible interaction with CDHA, which is a suitable model drug for our system. It should be incorporated into the CDHA/CS matrices in advance for diffusion exponent determination. The preparations of drug-loaded matrix membranes were similar to the above-mentioned process (Section 2.1). Before membrane drying, vitamin B_{12} was added into those CDHA/CS suspensions. The subsequent drying process was also the same as the above-mentioned process (Section 2.1). These composite membranes were put into phosphate-buffered solution (PBS, pH 7.4) for release test. The release medium was withdrawn for each juncture and replaced with equivalent volume of fresh buffer. UV–Visible spectroscopy (Agelent 8453) was used for the characterization of absorption peak at 361 nm to determine the amount of vitamin B_{12} released via the use of predetermined standard concentration–intensity calibration curve. The diffusion exponent (n) of non-porous material can be

Table 1
Synthetic conditions of the CDHA/CS nanocomposites

Processes	CDHA content	Composite code
In situ processes	5%	In situ 5
$H_3PO_4 \rightarrow CS \rightarrow Ca(CH_3COO)_2$	10%	In situ 10
	30%	In situ 30
	50%	In situ 50
Ex situ processes CS→CDHA	5%	Ex situ 5
	10%	Ex situ 10
	30%	Ex situ 30
	50%	Ex situ 50

determined by plotting $\mathrm{Log}(M_t/M_8) - \mathrm{Log}(t)$ curve and the use of Eq. (1):

$$(M_t/M_\infty) = kt^n \quad (1)$$

where M_t is the amount of drug released at time t, M_∞ is the amount of drug released at equilibrium state, k is a constant and n is the diffusion exponent related to the diffusion mechanism.

2.4. Determination of permeability of membrane system

The permeation tests were performed by the use of side-by-side diffusion cell. Vitamin B_{12} aqueous solution (90 ml) of 0.02% (m/v) was added into the donor cell as the model drug. The same volume of PBS was added into the receptor cell. Drug-free composite membrane was fixed between the two half-cells. The amount of vitamin B_{12} permeated was determined using UV–Visible spectroscopy for each juncture. Membrane permeability of polymeric film can be determined using Eq. (2) [19]:

$$\mathrm{Ln}(1 - C_t/C_0) = -(2ADH/V) = -(2AP/V) \quad (2)$$

where C_t is the solution concentration in the receptor cell at time t, C_0 is the initial solute concentration of the donor cell, V is the volume of each half-cell, A is the effective area of permeation, D is the diffusion coefficient, H is the partition coefficient, and P is the membrane permeability ($P = D * H$). The slope of the plot of $-((V/2A)\ \mathrm{Ln}\ (1 - C_t/C_0))$ versus t is membrane permeability. The apparent partition coefficient (H) of vitamin B_{12} for nanocomposite/aqueous medium was determined as follows [20]. Drug-free CDHA/CS nanocomposite (10 mg) was immersed in the release medium until equilibrium state. The wet weight (W) was recorded. The nanocomposite was then immersed in 10 ml of vitamin B_{12}-containing medium. Partition coefficient (H) was determined from the initial (C_0) and equilibrium (C_e) concentrations of vitamin B_{12}-containing mediums by Eq. (3):

$$H = 10(C_0 - C_e)/WC_e. \quad (3)$$

3. Results and discussion

3.1. Material characterization

Fig. 1 shows the cross-sectional area (fracture surface) of those composite membranes. For the in situ process (Fig. 1a–c), it can be found that most of the membranes were non-porous with dimple-like fractured surface except for the sample In situ

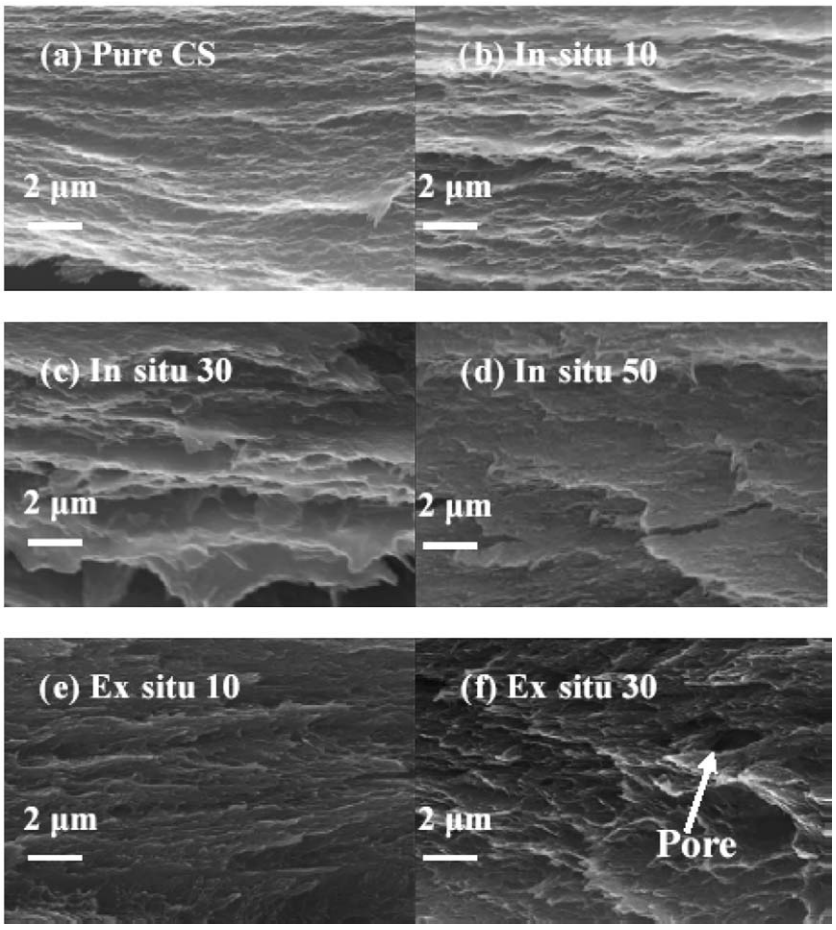

Fig. 1. Selective SEM micrographs (cross-section) of CDHA/CS nanocomposite membranes.

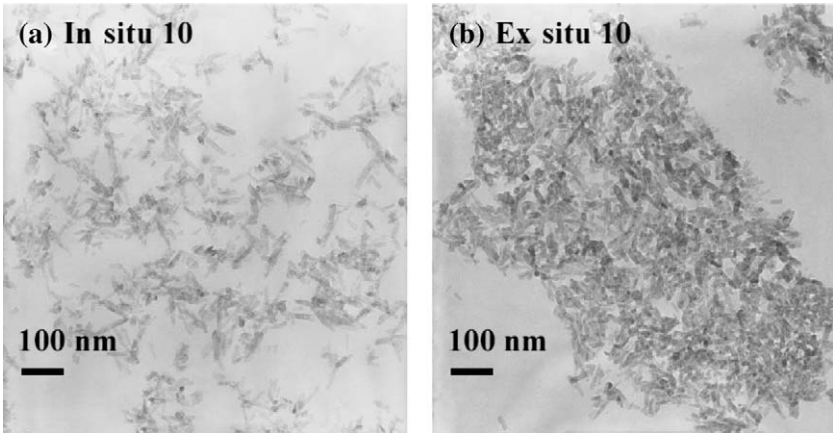

Fig. 2. Selective TEM micrographs of CDHA/CS nanocomposite membranes.

50 (Fig. 1d), which is probably caused by plastic deformation. The number of dimples decreased and the dimple size increased with increasing CDHA content. By contrast, for the ex situ process, the membranes became porous when the CDHA amount exceeded 30% (Fig. 1f). It is attributed to agglomeration of the incorporated CDHA nanoparticles that could be observed for the sample prepared via the ex situ route and evidenced by TEM as shown in Fig. 2. These agglomerates could be the favorable sites for the nucleation of voids upon drying. Therefore, in this work, data of Ex situ 30 and Ex situ 50 were excluded due to their macroporous structure, which could not comply with the fundamental hypothesis of Eqs. (1) and (2) in the forthcoming analysis [9].

Fig. 3 shows the XRD patterns of CDHA, CS and CDHA/CS nanocomposites. One major peak at $2\theta \sim 21°$ and two minor peaks at $2\theta \sim 26°$ and 32° appeared in both samples In situ 10 and Ex situ 10. According to the ICDD No. 39-1894 and No. 46-0905, the major peak and two minor peaks can be identified as semi-crystalline chitosan and poorly crystalline CDHA, respectively. It indicated that CDHA/CS composites could be synthesized through both in situ and ex situ processes. Furthermore, it was found that the crystallinity of CS was decreased with increasing CDHA content, which is probably caused by the well-dispersed CDHA nano-crystals which act as point defects in the chitosan matrix [15]. In addition, Strawhecker et al. also reported that strong polymer–filler interaction could change the molecular conformation of polymer chain in the vicinity of filler and simultaneously gave rise to the formation of localized amorphous regions [16]. This accounts for considerable inhibition of the crystallinity development of chitosan crystals and this retardation becomes more pronounced when the CDHA content exceeds 30 wt.%.

Fig. 4 shows the TGA curves of CDHA/CS nanocomposite membranes prepared via the in situ process. The TGA curve of Ex situ 10 was similar to that of In situ 5 (not shown). Thermal decomposition of pure chitosan without cross-link was clearly observed from 150 to 250 °C, which is attributed to the cleavage of hydrogen bonding [21]. However, no thermal decomposition region was observed for both In situ 30 and In situ 50. Furthermore, it was found that as the pure chitosan membrane was fully cross-linked by tripolyphosphate (TPP), its TGA curve was very similar to that of both In situ 30 and In situ 50. This result suggests that the CDHA acts as a cross-linking medium with chitosan, which is attributed to the electrostatic

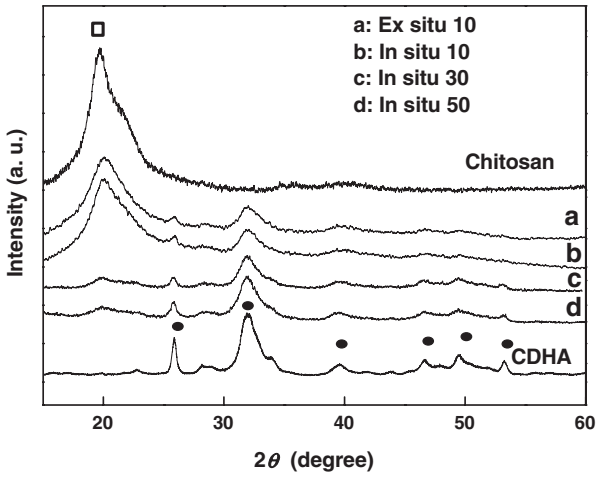

Fig. 3. XRD patterns of CS, CDHA and CDHA/CS nanocomposites.

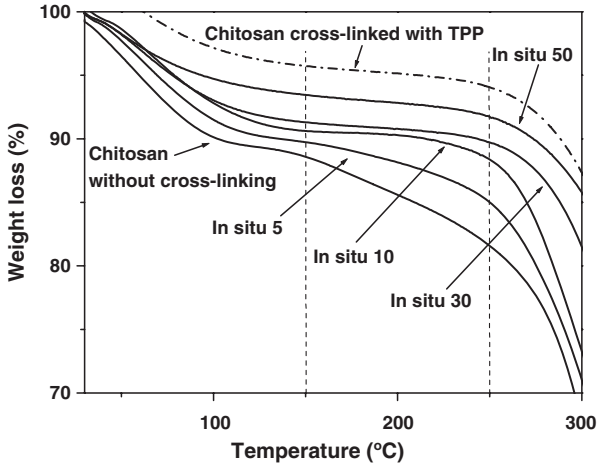

Fig. 4. TGA curves of TPP cross-linked chitosan and CDHA/CS nanocomposite membranes prepared via in situ process.

attraction between $(PO_4)^{3-}$ moieties (from CDHA) and protonated amino groups (NH_3^+) in chitosan molecules. This filler–polymer attraction force stabilizes the polymer chain network via the cross-linking operation. The degree of cross-link could be quantified by calculating the weight loss of the composite membranes with respect to the weight loss of pure chitosan in the range from 150 to 250 °C and the results are shown in Fig. 5a. As can be seen, when the incorporated CDHA was below 10%, the degree of cross-link increased almost linearly with CDHA content; above that, the correlation tended to become constant. This observation could be accounted for by assuming that all the NH_3^+ groups in chitosan molecules are fully occupied by interaction with the surface phosphate groups of the CDHA nanoparticles and under such a full occupation, no further sites are available for cross-link. On the other hand, for the sample with 10% CDHA, the degree of cross-link of the composite membrane prepared via the in situ process was higher than that synthesized via the ex situ process. It is then reasonable to believe that in situ synthesis offers more nucleation sites (i.e., filler–polymer interaction sites), resulting in better dispersion of the CDHA nanoparticles in the chitosan matrix (Fig. 2). Under this condition, the well-dispersed CDHA nano-crystals provide higher cross-link density (degree) with chitosan than that of the agglomerated CDHA nano-crystals prepared via the ex situ process.

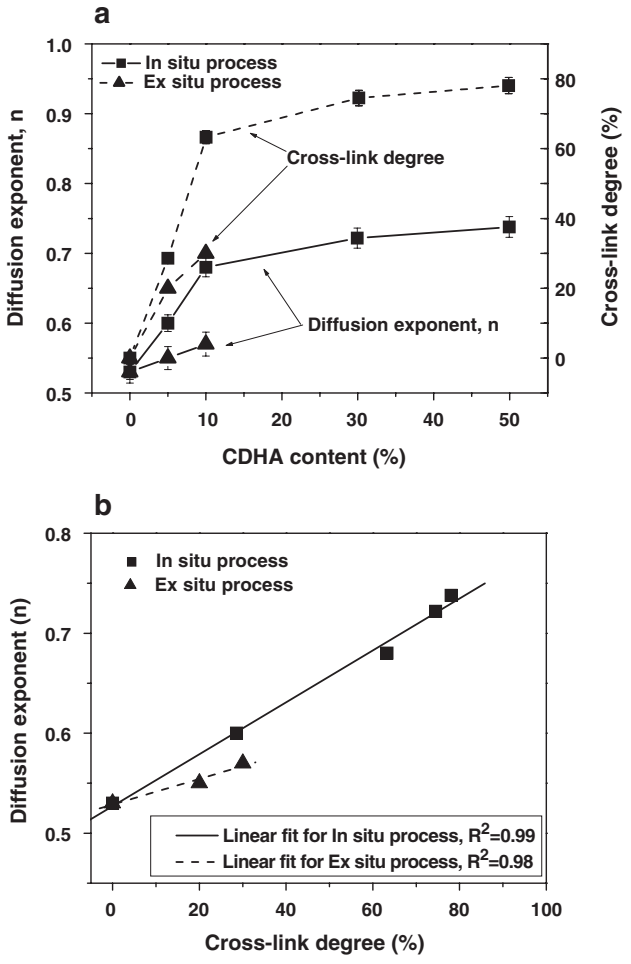

Fig. 5. a. Dependences of synthetic processes and amount of CDHA on the degree of cross-link and diffusion exponent of nanocomposite membranes. b. Dependences of degree of cross-link on the diffusion exponents of nanocomposite membranes.

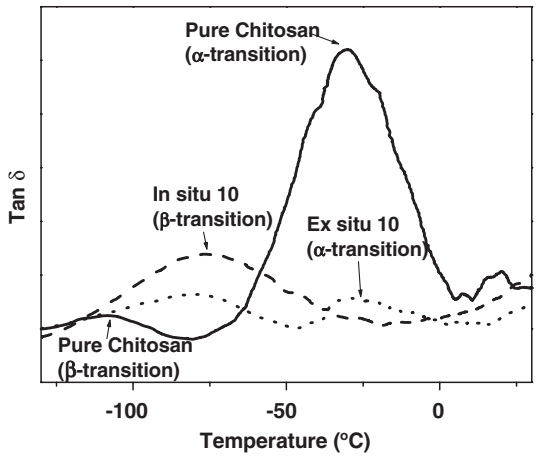

Fig. 6. DMA curves of chitosan and CDHA/CS nanocomposite membranes with CDHA content of 10%.

3.2. Diffusion exponent of drug-loaded matrix system

Diffusion exponent (n), as defined in Eq. (1), can be employed to determine release kinetics and diffusion mechanism for polymeric matrix drug delivery systems (DDS) [22,23]. As revealed in Fig. 5a, the exponent n was strongly affected by the synthetic process and concentration of the nanofiller. It was observed that the n values of the membranes synthesized through the in situ process were higher than those through the ex situ process. This, according to previous argument, is probably due to the stronger filler–polymer interaction (short-range interaction) between well-dispersed CDHA crystals and CS side groups, as well as chain–chain interaction (long-range interaction) in highly cross-linked network particularly for the in situ route. This assumption is further supported by DMA curves shown in Fig. 6. It is known that for semi-crystalline polymers, short-range interaction in the side group causes a shift of β-transition to the higher temperature region. Long-range interaction in backbone causes the α-transition to be broadened or even the peak to disappear [11,12,15]. These two phenomena were both observed in the DMA curves for sample In situ 10. It suggests that well-dispersed CDHA nanoparticles, i.e., in situ route, provide greater extent of interaction with the chitosan and reduce more effectively the molecular relaxation rate of chitosan molecules, i.e., restricted relaxation. This restriction of molecular relaxation is believed to affect drug diffusion within the nanocomposites and result in an increase in exponent n, indicating that drug release shifts from a diffusion-controlled towards swelling-controlled mechanism [23].

Hongbin et al. reported a coarse-grained domain relaxation model for depicting the restricted relaxation behaviour in the nanocomposite system according to the nature of polymer–filler interaction [14]. The polymer chains around the filler can be

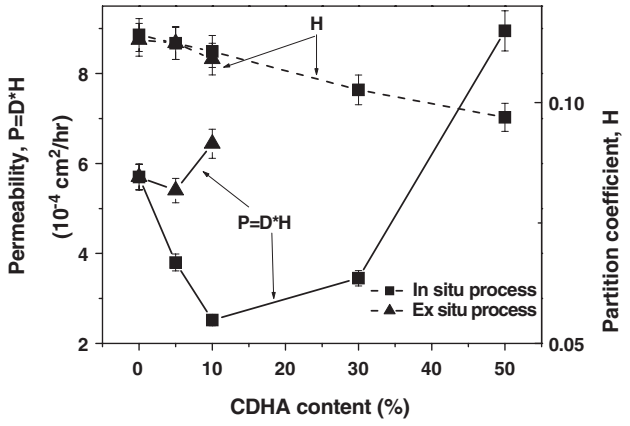

Fig. 7. Dependences of synthetic processes and CDHA content on the permeability (P) and partition coefficient (H) of CDHA/CS nanocomposite membranes.

classified into three regions: Domain I (slow relaxation region in the vicinity of filler), Domain II (fast relaxation region in the central areas among neighboring fillers), and Domain III (normal relaxation region in the bulk matrix). This model supports that α-transition peak with a lower peak height assigned to Domain III could be observed for sample Ex situ 10 (Fig. 6) because the total volume of Domain III is increased with the agglomeration of CDHA nanofillers in the CS matrix. Therefore, restricted molecular relaxation in the membrane prepared via the ex situ process is not as prominent as that prepared via the in situ process. Therefore, the diffusion exponent of the CDHA/CS membranes is lower for that synthesized through the ex situ processes than that through the in situ synthesis, as further confirmed in Fig. 5a.

The effect of CDHA content on diffusion exponent is illustrated in Fig. 5a. For pure CS, n was close to 0.5, indicating a Fickian diffusion kinetics. Incorporating the CDHA nanoparticles into CS matrices caused an increased n, which is well explained in terms of the coarse-grained domain relaxation model. Increasing the concentration of CDHA gives rise to an increase in polymer–filler interaction, leading to an increased volume of Domain I, and at the same time, a decrease in the volume of Domain II and Domain III. This indicates that the extent of restricted relaxation is increased when the concentration of CDHA increases. Therefore, when the CDHA was added up to 10%, exponent n was rapidly increased to 0.7 for the nanocomposite prepared via the in situ process, indicating a transition from diffusion control to swelling control. Furthermore, from experimental findings, when the CDHA was increased from 10% to 30%, the volume for Domains II and III was largely replaced by Domain I and tended to approach a saturated level. The n value then became relatively constant when the CDHA content exceeded 30%. Interestingly, this phenomenon reveals that the effect of CDHA content on diffusion exponent n is very similar to that of CDHA content on the degree of cross-link. This also implies a possible correlation of diffusion exponent with the degree of cross-link. Fig. 5b shows the resulting dependence, where a linear correlation with R^2 as high as 0.98 was obtained. It indicates that the degree of cross-link within the matrix due to the incorporation of CDHA nanoparticle affects profoundly the drug diffusion exponent.

3.3. Permeability of membrane system

The effect of CDHA content on the permeability and partition coefficient of the membrane prepared through the in situ process is illustrated in Fig. 7. It was found that the partition coefficient was slightly decreased with increasing CDHA content because the incorporated CDHA does not dissolve the model drug. It suggests that the diffusion coefficient (D) becomes the dominant item for membrane permeability ($P=D*H$). The membrane permeability was decreased with the incorporation of CDHA from 0% to 10%. However, further increase in the CDHA from 10% to 30% caused an increase in the permeability, which became more pronounced when the CDHA content was higher than 30%. These results may be explained as follows. The degree of cross-link and the length of diffusion path increase with the incorporation of CDHA nanofillers, leading to a decrease in diffusion coefficient. Therefore, the membrane permeability of CDHA/CS nanocomposite decreased with increasing CDHA content. On the contrary, the crystallinity decreased as CDHA was incorporated into the chitosan matrix as evidenced in Fig. 3. The CDHA nanoparticles retard the crystallization of chitosan, thus making the resulting chitosan more amorphous, which in turn increases the diffusion coefficient of the chitosan matrix [24]. Therefore, the influence of the CDHA on the chitosan diffusion coefficient is essentially a compromise between degree of cross-link and crystallinity. As the CDHA content was increased to over 30%, the decrease in crystallinity of the chitosan became dominant. In addition, a further addition of CDHA causes the agglomeration of nanoparticles as observed in sample In situ 50, which may further induce the formation of microcracks between the CDHA phase and the chitosan matrix as a result of increased rigidity or more specifically, voids within the CDHA agglomerates. Either microcracks or voids could act as effective diffusion paths, which cause a significant increase in permeability, as observed in sample In situ 50.

Fig. 7 also shows the influence of synthetic processes on membrane permeability. For the CDHA content of 5% and 10%,

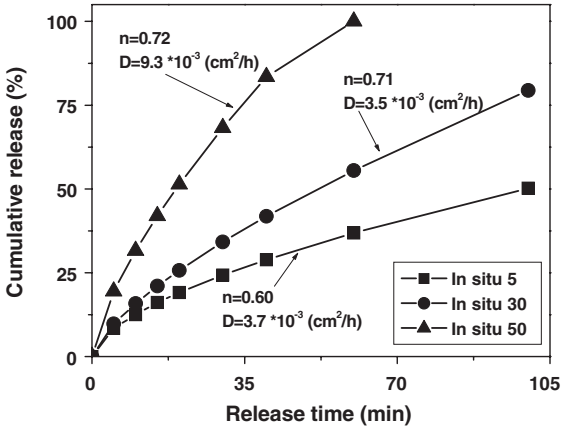

Fig. 8. Release profiles of CDHA/CS nanocomposite matrix membranes.

the permeability of composite membranes was lower for the in situ route than that via the ex situ process. This is probably due to better dispersion of the CDHA nanoparticles for samples prepared by the in situ process, resulting in more efficient physical barriers. A higher degree of cross-link (Fig. 5a), compared with the ex situ synthesis, also provides inhibition to the resulting diffusion coefficient.

According to the aforementioned argument, it is possible to manipulate the release profile by selecting suitable values of n and P through incorporating various contents of CDHA. Take 5%, 30% and 50% for example, the resulting drug release profiles for vitamin B_{12} from the matrix membranes are illustrated in Fig. 8. A near-zero order release profile with rapid release rate was observed for the 50% (In situ 50) matrix membrane samples (with $n=0.72$, $P=8.9*10^{-4}\,cm^2/h$, $H=0.096$, $D=9.3*10^{-3}\,cm^2/h$); however, a near-zero order release profile with moderate release rate was achieved for the 30% ones (with $n=0.71$, $P=3.4*10^{-4}\,cm^2/h$, $H=0.103$, $D=3.5*10^{-3}\,cm^2/h$). It suggests that D value could be altered drastically without changing the n value for CDHA amount ranging from 30% to 50%. Compared with In situ 30, In situ 5 had a relative long-term release (with $n=0.6$, $P=3.7*10^{-4}\,cm^2/h$, $H=0.112$, $D=3.7*10^{-3}\,cm^2/h$), whose D value was close to that of In situ 30.

Recently, sequential release of growth factor has been reported because of its potential in enhancing wound healing and osteogenesis [25]. In addition, using combination antibiotic therapy to decrease antibiotic-resistance has been investigated [26,27]. Therefore, it is feasible to design a bone substitute consisting of CDHA/CS composite loaded with multiple drugs for either simultaneous release or sequential release via regulating the amount of CDHA nano-phase [28]. Compared with existing conventional approaches to manipulating drug release kinetics (i.e., molecular weight, crystallinity, amount of cross-linking agents), this study provides a relatively simple, precise and controllable synthetic methodology for manipulating release kinetics. In this work, in order to clarify the effect of filler–polymer on drug release kinetics, vitamin B_{12} was selected as the model drug because of its small molecular weight, as well as negligible drug–filler and drug–polymer interaction. Unfortunately, a variety of bioactive agents with a wide range of drug–filler interaction, drug–polymer interaction and molecular weight may be therapeutically inconsistent or possibly interacted adversely in the same carrier materials, which merits further investigation.

4. Conclusions

In conclusion, an orthopedic implant material consisting of chitosan and CDHA with drug delivery function has been studied. It was found that both the amount of CDHA incorporated and the synthetic process altered significantly the extent of filler–polymer interaction, which influences strongly the diffusion exponent and permeability of CDHA/chitosan nanocomposites. Hence, CDHA nanocrystal could concurrently play the roles as bioactive nanofiller and drug-release regulator. This study may provide valuable information for a better design of chitosan-based orthopedic devices with improved bioactivity and controlled drug release function.

Acknowledgement

The authors gratefully acknowledge the National Science Council of the Republic of China for its financial support through Contract No. NSC-93-2216-E-009-027. Thanks also go to ApaMatrix Technologies Inc, Canada, for technical support.

References

[1] F. Zhao, Y. Yin, W.W. Lu, J.C. Leong, W. Zhang, J. Zhang, M. Zhang, K. Yao, Preparation and histological evaluation of biomimetic three-dimensional hydroxyapatite/chitosan–gelatin network composite scaffolds, Biomaterials 23 (2002) 3227–3234.
[2] G.S. Sailaja, S. Velayudhan, M.C. Sunny, K. Sreenivasan, H.K. Varma, P. Ramesh, Hydroxyapatite filled chitosan–polyacrylic acid polyelectrolyte complexes, J. Mater. Sci. 38 (2003) 3653–3662.
[3] J.S. Ahn, H.K. Choi, M.K. Chun, J.M. Ryu, J.H. Jung, Y.U. Kim, C.S. Cho, Release of triamcinolone acetonide from mucoadhesive polymer composed of chitosan and poly(acrylic acid) in vitro, Biomaterials 23 (2002) 1411–1416.
[4] M. Ito, Y. Hidaka, M. Nakajima, H. Yagasaki, A.H. Kafrawy, Effect of hydroxyapatite content on physical properties and connective tissue reactions to a chitosan–hydroxyapatite composite membrane, J. Biomed. Mater. Res. 45 (1999) 204–208.
[5] Y.J. Yin, F. Ye, J.F. Cui, F.J. Zhang, X.L. Li, K.D. Yao, Preparation and characterization of macroporous chitosan–gelatin beta-tricalcium phosphate composite scaffolds for bone tissue engineering, J. Biomed. Mater. Res. A 67 (2003) 844–855.
[6] M. Geiger, R.H. Li, W. Friess, Collagen sponges for bone regeneration with rhBMP-2, Adv. Drug Deliv. Rev. 55 (2003) 1613–1629.
[7] F. Chen, Z.C. Wang, C.J. Lin, Preparation and characterization of nano-sized hydroxyapatite particles and hydroxyapatite/chitosan nano-composite for use in biomedical materials, Mater. Lett. 57 (2002) 858–861.
[8] I. Yamaguchi, S. Iizuka, A. Osaka, H. Monmad, J. Tanaka, The effect of citric acid addition on chitosan/hydroxyapatite composites, Colloids Surf., A Physicochem. Eng. Asp. 214 (2003) 111–118.
[9] R. Langer, Polymeric delivery system for controlled drug release, Chem. Eng. Commun. 6 (1980) 1–48.
[10] L.H. Sperling, Introduction to Physical Polymer Science, Second edition, John Wiley and Sons, New York, 1992, pp. 148–149.
[11] K. Kesenci, L. Fambri, C. Migliaresi, E. Piskin, Preparation and properties of poly(L-lactide)/hydroxyapatite composites, J. Biomater. Sci., Polym. Ed. 11 (2000) 617–632.
[12] V. Arrighi, I.J. McEwen, H. Qian, M.B. Serrano Prieto, The glass transition and interfacial layer in styrene-butadiene rubber containing silica nanofiller, Polymer 44 (2003) 6259–6266.
[13] H.W. Goh, S.H. Goh, G.Q. Xu, K.P. Pramoda, W.D. Zhang, Dynamic mechanical behavior of in situ functionalized multi-walled carbon nanotube/phenoxy resin composite, Chem. Phys. Lett. 373 (2003) 277–283.
[14] H. Lu, S. Nutt, Restricted relaxation in polymer nanocomposites near the glass transition, Macromolecules 36 (2003) 4010–4016.
[15] Y.Q. Huang, Y.Q. Zhang, Y.Q. Hua, Studies on dynamic mechanical and rheological properties of LLDPE/nano-SiO_2 composites, J. Mater. Sci. Lett. 22 (2003) 997–998.
[16] K.E. Strawhecker, E. Manias, Crystallization behavior of poly(ethylene oxide) in the presence of Na^+ montmorillonite fillers, Chem. Mater. 15 (2003) 844–849.
[17] B.J. Ash, L.S. Schadler, R.W. Siegel, Glass transition behavior of alumina/polymethylmethacrylate nanocomposites, Mater. Lett. 55 (2002) 83–87.
[18] Q. Hu, B. Li, M. Wang, J. Shen, Preparation and characterization of biodegradable chitosan/hydroxyapatite nanocomposite rods via in situ hybridization: a potential material as internal fixation of bone fracture, Biomaterials 25 (2004) 779–785.

[19] N.A. Peppas, N.M. Franson, The swelling interface number as a criterion for prediction of diffusional solute release mechanism in swellable polymers, J. Appl. Polym. Sci. 21 (1983) 983–997.
[20] M. Miyajima, A. Koshika, J. Okada, M. Ikeda, Mechanism of drug release from poly(L-lactic acid) matrix containing acidic or neutral drugs, J. Control. Release 60 (1999) 199–209.
[21] C.L. Tien, M. Lacroix, P. Ispas-Szabo, M.A. Mateescu, *N*-acylated chitosan: hydrophobic matrices for controlled drug release, J. Control. Release 93 (2003) 1–13.
[22] N.A. Peppas, Analysis of Fickian and non-Fickian drug release from polymers, Pharm. Acta Helv. 60 (1985) 110–111.
[23] N.A. Peppas, R.W. Korsmeyer, Dynamically swelling hydrogels in controlled release applications, in: N.A. Peppas (Ed.), Hydrogels in Medicine and Pharmacy, vol. 3, CRC Press, Boca Raton, 1986, pp. 109–136.
[24] J. Seo, H. Han, Water diffusion studies in polyimide thin films, J. Appl. Polym. Sci. 82 (2001) 731–737.
[25] A.T. Raiche, D.A. Puleo, In vitro effects of combined and sequential delivery of two bone growth factors, Biomaterials 25 (2004) 677–685.
[26] M. Tatman-Otkun, S. Gurcan, B. Ozer, N. Shokrylanbaran, Annual trends in antibiotic resistance of nosocomial *Acinetobacter baumannii* strains and the effect of synergistic antibiotic combinations, Microbiologica 27 (2004) 21–28.
[27] Y.W. Miller, E.A. Eady, R.W. Lacey, J.H. Cove, D.N. Joanes, W.J. Cunliffe, Sequential antibiotic therapy for acne promotes the carriage of resistant staphylococci on the skin of contacts, J. Antimicrob. Chemother. 38 (1996) 829–837.
[28] M. Borden, S.F. El-Amin, M. Attawia, C.T. Laurencin, Structural and human cellular assessment of a novel microsphere-based tissue engineered scaffold for bone repair, Biomaterials 24 (2003) 597–609.